

Multi-Criterial Design of Antennas with Tolerance Analysis Using Response-Feature Predictors

Anna Pietrenko-Dabrowska¹[0000-0003-2319-6782], Slawomir Koziel^{1,2}[0000-0002-9063-2647],
and Leifur Leifsson³[0000-0001-5134-870X]

¹ Faculty of Electronics Telecommunications and Informatics, Gdansk University of Technology, Narutowicza 11/12, 80-233 Gdansk, Poland
anna.dabrowska@pg.edu.pl

² Engineering Optimization & Modeling Center, Department of Engineering, Reykjavik University, Menntavegur 1, 102 Reykjavik, Iceland
koziel@ru.is

³ School of Aeronautics and Astronautics, Purdue University, West Lafayette, IN 47907, USA
leifur@purdue.edu

Abstract. Imperfect manufacturing is one of the factors affecting the performance of antenna systems. It is particularly important when design specifications are strict and leave a minimum leeway for a degradation caused by geometry or material parameter deviations from their nominal values. At the same time, conventional antenna design procedures routinely neglect to take the fabrication tolerances into account, which is mainly a result of a challenging nature of uncertainty quantification. Nevertheless, the ability to assess the effects of parameter deviations and to mitigate thereof is instrumental in achieving truly robust antenna designs. Furthermore, identifying the antenna-specific relationships between nominal requirements and tolerance immunity is essential to determine the necessary levels of fabrication accuracy, which affects both the reliability and the manufacturing costs. This paper proposes a technique for multi-criterial optimization of antenna structures oriented towards rendering a family of designs representing trade-offs between the nominal performance and the robustness. The fundamental components of our procedure are feature-based regression models constructed at the level of selected characteristic points of the antenna outputs. The trade-off designs are generated sequentially, using local search carried out for gradually relaxed nominal requirements. Numerical experiments conducted for two microstrip antennas demonstrate that the proposed algorithm is capable of yielding the performance/robustness Pareto set at the cost of only a few dozens of EM analysis of the antenna at hand per design, while ensuring reliability, as validated by means of EM-based Monte Carlo simulation.

Keywords: Antenna design, multi-criterial optimization, simulation-based design, manufacturing tolerances, statistical analysis, response features.

1 Introduction

Manufacturing processes such as chemical etching or mechanical milling are of finite resolution and accuracy, whereas our knowledge of material parameters (e.g., substrate permittivity) and operating conditions (e.g., input power level, temperature) is always limited. At the same time, the aforementioned uncertainties, especially deviations of geometry parameters from their nominal values, may be detrimental to the electrical and field characteristics of antennas [1]. In order to meet the stringent performance demands imposed on contemporary radiating structures, the design process should account for the effects of uncertainties to ensure that the system operates properly even under the most pessimistic scenarios.

In practical terms, the improvement of antenna performance requires utilization of numerical optimization methods [2]-[4]. At the same time, for the sake of reliability, parameter tuning is normally carried out using full-wave electromagnetic (EM) simulation models, which incurs considerable computational expenses. These are especially high in the case of global search procedures [5]-[7]. If the design process is to account for both the nominal performance and the effects of fabrication tolerances, in particular, if performance-robustness trade-offs are of interest, multi-objective optimization (MO) becomes imperative. MO is a CPU-heavy endeavor. The most popular acceleration methods involve surrogate modeling techniques [8], [9], both data-driven (kriging [10], support-vector regression [11]) or physics-based (e.g., space mapping [12], sequential domain patching [13]), often combined with machine-learning methodologies [14].

Quantification of the effects of fabrication tolerances requires appropriate statistical performance metrics. In the case of antennas, it is usually the yield [15], which is a likelihood of satisfying given performance requirements under the assumed probability distributions that govern deviations of the antenna parameters. Consequently, robust design techniques are mainly concerned with yield improvement [16], [17]. The alternative is to seek for the maximum allowed levels of input tolerances, for which the system outputs remain acceptable (maximum input tolerance hypervolume, MITH [18]). Unfortunately, estimation of the yield is a computationally expensive process. For example, EM-driven Monte Carlo (MC) simulation typically requires hundreds of EM analyses. Most of state-of-the-art statistical analysis methods rely on surrogate modeling methods [19]-[21], with a notable example of polynomial chaos expansion (PCE) [22]. Yet, handling higher-dimensional problems is still an issue due to considerable initial cost of surrogate model construction. A possible way of alleviating these difficulties is performance-driven modeling [23].

The literature offers few methods for multi-objective antenna design with tolerance analysis. For example, in [24], kriging surrogates are employed along with the worst-case analysis at the Pareto-optimal designs found by means of the particle swarm optimization algorithm. Machine-learning approach involving Gaussian Process Regression surrogates has been reported in [25], whereas [26] is the only methods that explicitly handles input tolerance hypervolume as one of the design objectives. In all cases, low-dimensional parameter spaces are considered.

This paper introduces a novel surrogate-based algorithm for low-cost tolerance-aware multi-objective design of antenna structures. In our methodology, maximization of the input tolerance levels for which the design specifications are still met is treated as one of the explicit objectives, the other being nominal performance of the antenna at

hand. The optimization process is expedited through the employment of feature-based regression models, rendered at the level of suitably chosen characteristic points of antenna responses. The Pareto-optimal designs are identified sequentially for the selected values of relevant performance figures, using local gradient-based tuning. The presented technique is demonstrated using two microstrip antennas, and shown to be both reliable and computationally efficient with the CPU cost of generating trade-off designs as low as a few dozens of EM simulations per point.

2 Multi-Criterial Antenna Optimization with Tolerance Analysis

This section introduces the proposed multi-objective optimization strategy with tolerance analysis. Formulation of the design task is followed by an exposition of the statistical analysis approach, a description of the procedure for identifying the trade-off designs, as well as a summary of the entire MO framework.

2.1 Problem Formulation

We denote by $\mathbf{R}(\mathbf{x})$ the antenna responses corresponding to the parameter vector $\mathbf{x} = [x_1 \dots x_n]^T$, and obtained through full-wave EM analysis. We will also use additional symbols to denote specific frequency characteristics such as reflection $S_{11}(\mathbf{x}, f)$, axial ratio $AR(\mathbf{x}, f)$, or gain $G(\mathbf{x}, f)$, where f stands for the frequency. The function $F_p(\mathbf{x})$ will be used to denote the nominal performance for the antenna, i.e., assuming no fabrication tolerances.

Consider a multi-band antenna with the target operating frequencies f_{0k} , $k = 1, \dots, N$, and target bandwidths B_k . The design specifications are defined for a performance parameter $P(\mathbf{x}, f)$, which should not exceed the value of P_{\max} over the bandwidths of interest. In other words, the specifications are satisfied if

$$\max \left\{ f \in \bigcup_{k=1}^N [f_{0k} - B_k, f_{0k} + B_k] : |P(\mathbf{x}, f)| \leq P_{\max} \right\} \quad (1)$$

For example, if $P(\mathbf{x}, f) = |S_{11}(\mathbf{x}, f)|$ (antenna input characteristics), the acceptable level is typically set to $P_{\max} = S_{11.\max} = -10$ dB.

The best nominal design \mathbf{x}^p is obtained by improving the performance parameter P as much as possible over the target bandwidths, i.e., we have

$$\mathbf{x}^p = \arg \min_{\mathbf{x}} \left\{ \max \left\{ f \in \bigcup_{k=1}^N [f_{0k} - B_k, f_{0k} + B_k] : P(\mathbf{x}, f) \right\} \right\} \quad (2)$$

According to (2), the target nominal antenna performance $F_p(\mathbf{x})$ is simply P_{\max} .

Let $F_r(\mathbf{x})$ be a function representing the antenna design robustness. In this work, we assume that parameter deviations follow independent Gaussian distributions of zero mean and a variance σ (the same for all parameters); generalization of arbitrary distributions is straightforward. We define $F_r(\mathbf{x}) = \sigma(\mathbf{x})$, where the dependence on the design \mathbf{x} emphasizes the fact that the maximum allowed variance is a function of antenna parameters. The meaning of F_r is that—at design \mathbf{x} —it is the maximum value of the variance σ , for which the performance specifications are still satisfied for any design perturbed with respect to \mathbf{x} , with the perturbations not larger than 3σ .

The tolerance-aware multi-objective optimization task can be then formulated as

$$\mathbf{x}^* = \arg \min_{\mathbf{x}} [F_p(\mathbf{x}) - F_r(\mathbf{x})] \quad (3)$$

Thus, the objective is to improve both the nominal performance $F_p(\mathbf{x})$ and the robustness $F_r(\mathbf{x})$. Note that both objectives are conflicting as imposing more demanding target nominal performance leads to a reduced robustness, because there is a smaller margin for parameter deviations left. We also have two extreme designs: (i) the best nominal design \mathbf{x}^p , and (ii) the minimum acceptable performance design \mathbf{x}^r . The latter corresponds to the highest target value of F_p that can be accepted for a given application (e.g., -10 dB in the case of reflection response). Also, \mathbf{x}^r is found by maximizing F_r given the aforementioned highest value of F_p . Here is a brief characteristic of the two designs:

- \mathbf{x}^p : as this design corresponds to the best nominal performance (e.g., the lowest in-band reflection of the antenna), it features the minimum robustness. In particular, the level of parameter deviations ensuring the fulfilment of performance specifications is zero because any deviation from the nominal values results in worsening of F_p ;
- \mathbf{x}^r : at this design, we have the largest performance margin w.r.t. the best nominal design \mathbf{x}^p . Thus, \mathbf{x}^r exhibits the largest robustness as the feasible region for the highest considered value of F_p is the largest.

The designs that are globally non-dominated in the Pareto sense [27] w.r.t. to F_p and F_r form the Pareto front X_P [27]. These are the best possible trade-offs between the nominal performance and the robustness. Our goal is to identify a discrete subset of X_P , distributed uniformly along the front. The concepts considered in this sections have been illustrated in Fig. 1.

2.2 Yield Estimation by Means of Response Features

The robustness $F_r(\mathbf{x})$ is defined to be the maximum value of the variance σ of Gaussian probability distributions characterizing the geometry parameter deviations, for which the fabrication yield retains 100 percent. The yield is defined as [28]

$$Y(\mathbf{x}) = \int_{X_f} p(\mathbf{y}, \mathbf{x}) d\mathbf{y} \quad (4)$$

In (4), $p(\mathbf{y}, \mathbf{x})$ is a probability density function describing statistical variations of the design \mathbf{y} w.r.t. the vector \mathbf{x} . The feasible space X_f contains the designs that meet the performance specifications (cf. (1)). As X_f is unknown explicitly, the yield is normally approximated through Monte Carlo (MC) simulation as

$$Y(\mathbf{x}) = N_r^{-1} \sum_{k=1}^{N_r} H(\mathbf{x} + d\mathbf{x}^{(k)}) \quad (5)$$

where $d\mathbf{x}^{(k)}$, $k = 1, \dots, N_r$, are generated using the function p . The function H equals 1 if the design specifications are satisfied, and zero otherwise. Evaluation of (5) is computationally expensive, therefore, surrogate modeling techniques are often used for the sake of accelerating the process [19]-[22]. The robustness metric $F_r(\mathbf{x}) = \sigma(\mathbf{x})$ is computed as

$$F_r(\mathbf{x}) = -\arg \max_{\sigma} \{Y(\mathbf{x}, \sigma) = 1\} \quad (6)$$

where the explicit dependence of Y on σ is to emphasize that the variance determines the input tolerance levels, which affect the yield.

Here, efficient evaluation of (6) is ensured by employing feature-based regression models described below. The response feature technology has been introduced in [29]

to accelerate antenna parameter tuning. The key idea is to reformulate the design task in terms of suitable chosen characteristic (or feature) points, e.g., frequency and level coordinates of antenna resonances, the coordinates of which are in weakly-nonlinear relationship with the antenna geometry parameters. This reformulation leads to a faster convergence of the optimization algorithms [30], as well as a reduced number of training data points when constructing surrogate models [31].

An illustration of the feature points for a reflection response of a triple band antenna can be found in Fig. 2. In the considered example, the points are defined to verify satisfaction of the performance specs imposed on the impedance matching of the device.

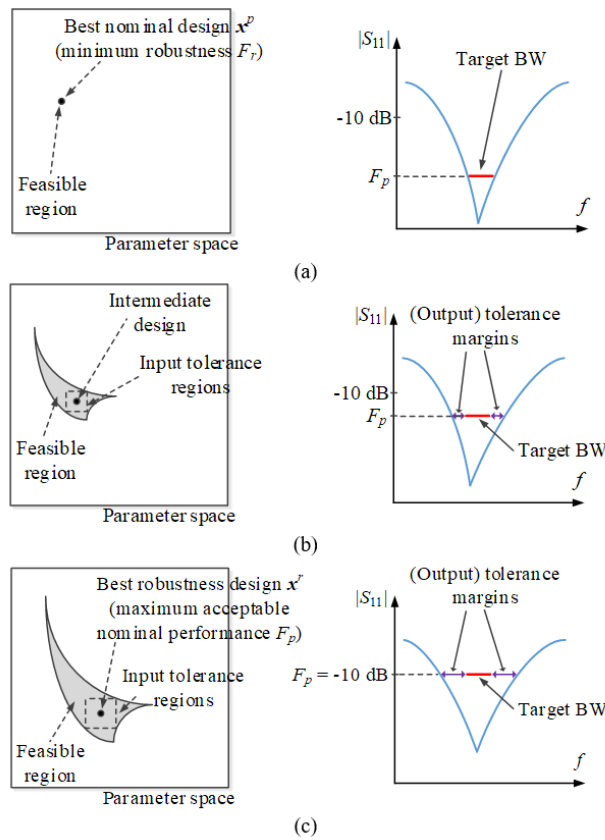


Fig. 1. Tolerance-aware multi-objective antenna design. A feasible region, shaded grey, contains designs satisfying performance requirements for a given F_p ; the region becomes larger when relaxing F_p . The right-hand-side plots show exemplary reflection responses vs. target impedance bandwidth for different levels of target nominal performance threshold F_p : (a) at the best nominal design x^p , the feasible region is a single point x^p , hence, the input tolerance level is zero; (b) for an intermediate design, the feasible region is larger and the most robust design is centred therein to maximize the input tolerance ranges ensuring performance requirements satisfaction; (c) for the most robust design, corresponding to the maximum acceptable level of F_p (e.g., -10 dB for $|S_{11}|$), the input tolerance levels are the largest upon concluding the optimization process. The family of designs obtained for different values of F_p form a Pareto set (performance vs. robustness trade-offs).

In relation to the performance requirements of (1), the feature vector $\mathbf{P}(\mathbf{x})$ at design \mathbf{x} is defined as

$$\mathbf{P}(\mathbf{x}) = [p_1(\mathbf{x}) \ p_2(\mathbf{x}) \ \dots \ p_{2N}(\mathbf{x})]^T = [f_1(\mathbf{x}) \ f_2(\mathbf{x}) \ \dots \ f_{2N}(\mathbf{x})]^T \quad (7)$$

Here, the frequencies f_{2k-1} and f_{2k} are such that $P(\mathbf{x}; f_{2k-1}) = P(\mathbf{x}; f_{2k}) = P_{\max}$ for the k th operating band, $k = 1, \dots, N$. The condition (1) can be reformulated using \mathbf{P} as

$$p_{2k-1}(\mathbf{x}) \leq f_{0,k} - B_k, \quad p_{2k}(\mathbf{x}) \geq f_{0,k} + B_k, \quad k = 1, \dots, N \quad (8)$$

As the dependence between the feature points and antenna geometry parameters is weakly nonlinear, the feature vector $\mathbf{P}(\mathbf{x})$ at the design \mathbf{x} located in a small vicinity of the current design $\mathbf{x}^{(i)}$ (produced in the course of the optimization process) can be predicted using a simple regression model. Here, we use a linear model $\mathbf{L}_P^{(i)}(\mathbf{x})$

$$\mathbf{L}_P^{(i)}(\mathbf{x}) = [p_{L,1}(\mathbf{x}) \ \dots \ p_{L,2N}(\mathbf{x})]^T = \begin{bmatrix} l_{0,1} + \mathbf{L}_1^T(\mathbf{x} - \mathbf{x}^{(i)}) \\ \vdots \\ l_{0,2N} + \mathbf{L}_{2N}^T(\mathbf{x} - \mathbf{x}^{(i)}) \end{bmatrix} \quad (9)$$

The model is identified using $n + 1$ training pairs $\{\mathbf{x}_B^{(j)}, \mathbf{P}(\mathbf{x}_B^{(j)})\}$, $j = 1, \dots, n+1$, arranged as follows: $\mathbf{x}_B^{(1)} = \mathbf{x}^{(i)}$, and $\mathbf{x}_B^{(j)} = \mathbf{x}^{(i)} + [0 \ \dots \ 0 \ d \ 0 \ \dots \ 0]^T$ (d on the $(j-1)$ th position). The distance parameter $d = 3\sigma$, where σ is the variance of the Gaussian distribution governing the antenna parameter deviations. The coefficients of $\mathbf{L}_P^{(i)}$ are found as

$$\begin{bmatrix} l_{0,j} \\ \mathbf{L}_j \end{bmatrix} = \begin{bmatrix} 1 & (\mathbf{x}_B^{(1)} - \mathbf{x}^{(i)})^T \\ \vdots \\ 1 & (\mathbf{x}_B^{(n+1)} - \mathbf{x}^{(i)})^T \end{bmatrix}^{-1} \begin{bmatrix} p_j(\mathbf{x}_B^{(1)}) \\ \vdots \\ p_j(\mathbf{x}_B^{(n+1)}) \end{bmatrix}, \quad j = 1, \dots, 2N \quad (10)$$

The robustness metric $F_r(\mathbf{x})$ of (6) is evaluated by numerically integrating (4) with the use of the regression model (9). As the condition (1) is equivalent to (8), the yield $Y(\mathbf{x}, \sigma)$ can be estimated using random observables $\mathbf{x}_r^{(j)}$ allocated using the probability distribution characterized by the variance σ . The yield evaluation procedure has been summarized in Fig. 3. All steps in the above algorithm of Fig. 3 are vectorized to speed up the process.

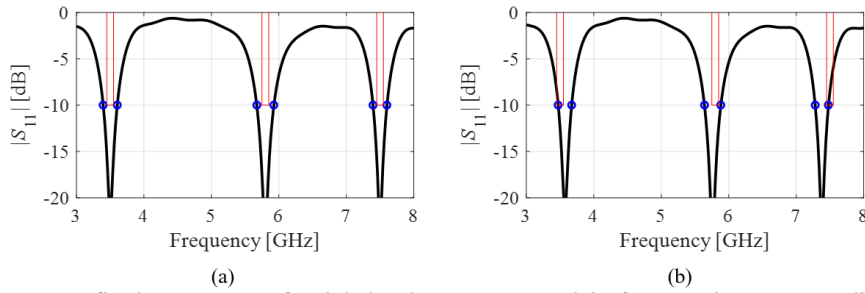


Fig. 2. Reflection responses of a triple-band antenna (—) and the feature points corresponding to -10 dB $|S_{11}|$ levels (o). Design specifications are shown using the thin lines. The frequency coordinates of the feature points allow us to determine satisfaction/violation of performance requirements imposed on impedance matching, here for $P_{\max} = -10$ dB (cf. (1)): (a) design satisfying specifications, (b) design violating specifications.

1. Input parameter: variance σ ;
2. Generate random observables $\{\mathbf{x}_r^{(j)}\}_{j=1, \dots, N_r}$;
3. Evaluate regression surrogate $L_p^{(j)}(\mathbf{x}_r^{(j)})$ for $j = 1, \dots, N_r$;
4. Evaluate (8) for all observables using predicted feature points $\rho_{L,k}(\mathbf{x}_r^{(j)})$, $j = 1, \dots, N_r$;
5. Estimate the yield $Y(\mathbf{x}, \sigma)$ as in (5).

Fig. 3. Evaluating the antenna yield using feature-based regression surrogate.

Having implemented the means for rapid estimation of the yield, the evaluation of F_r is carried out by solving (6) using golden ratio search [32] (note that given a joint variance σ , the task (6) is a one-dimensional problem). Should the probability distribution be determined by multiple parameters (e.g., a covariance matrix), the problem (6) can be solved by means of other methods, e.g., gradient-based algorithms.

2.3 Generating Trade-Off Designs

Our goal is to generate N_p trade-off designs, which form a discrete set of Pareto-optimal vectors w.r.t. the objectives F_p and F_r . Note that the Pareto front is spanned between the best nominal design \mathbf{x}^p , and the most robust design \mathbf{x}^r (cf. Section 2.1). The first trade-off design is therefore assigned as $\mathbf{x}^{(1)} = \mathbf{x}^p$, and it is obtained using (2). Consequently, the nominal objective function value $F_p(\mathbf{x}^{(1)})$, denoted as $P_{\max,1}$, is

$$P_{\max,1} = \max \left\{ f \in \bigcup_{k=1}^N [f_{0k} - B_k, f_{0k} + B_k] : P(\mathbf{x}^p, f) \right\} \quad (11)$$

In the next step, we set $P_{\max, NP} = P_{\max}$ (the maximum acceptable target level), which will determine the opposite end of the Pareto set. The $N_p - 1$ trade-off designs $\mathbf{x}^{(j)}$, $j = 2, \dots, N_p$, that remain to be generated will be obtained for the target levels $P_{\max, j}$, $j = 1, \dots, N_p$, uniformly distributed between $P_{\max,1}$ and $P_{\max, NP}$, i.e., we set

$$F_p(\mathbf{x}^{(j)}) = P_{\max, j} = P_{\max,1} + \left[P_{\max, NP} - P_{\max,1} \right] \frac{j-1}{N_p - 1} \quad (12)$$

This arrangement leads to equally-spaced trade-off designs w.r.t. the nominal performance objective F_p .

The designs $\mathbf{x}^{(j)}$, $j = 2, \dots, N_p$, are found as

$$\mathbf{x}^{(j)} = \arg \min_{\mathbf{x}} F_r(\mathbf{x}) \quad (13)$$

with P_{\max} in (8) set to $P_{\max, j}$. Solving (13) means that the antenna robustness, understood as in (6), is maximized for the (nominal) target value set to $P_{\max, j}$.

The problem (13) is solved using the trust-region (TR) framework [33], which produces a series of approximation $\mathbf{x}^{(j, i+1)}$ to $\mathbf{x}^{(j)}$ as

$$\mathbf{x}^{(j, i+1)} = \arg \min_{\|\mathbf{x} - \mathbf{x}^{(j, i)}\| \leq d^{(i)}} F_r(\mathbf{x}) \quad (14)$$

starting from $\mathbf{x}^{(j, 0)} = \mathbf{x}^{(j-1)}$. The search region size $d^{(i)}$ is adjusted based on standard TR rules [33]. The acceptance of a design $\mathbf{x}^{(j, i+1)}$ depends on the gain ratio

$$r = \frac{F_r^\#(\mathbf{x}^{(j, i+1)}) - F_r(\mathbf{x}^{(j, i)})}{F_r(\mathbf{x}^{(j, i+1)}) - F_r(\mathbf{x}^{(j, i)})} \quad (15)$$

which compares the actual improvement of the antenna robustness with the prediction

of the feature-based regression surrogate. Note that $F_r^\#$ in the numerator of (15) is calculated as in Section 2.2, but with $L_p^{(j,i)}$ replaced by the linear model $L_p^{\#(j,i)}$. The latter is constructed as in (9), (10) but with the coefficient vector $[l_{0.1} \dots l_{0.2N}]^T$ replaced by $\mathbf{P}(\mathbf{x}^{(j,i+1)})$. Using $F_r^\#$ enables low-cost evaluation of the gain ratio (only one EM simulation is involved). Although this is an approximation, it is justified by a typically small distance between $\mathbf{x}^{(j,i)}$ and $\mathbf{x}^{(j,i+1)}$, comparable to σ .

The vector $\mathbf{x}^{(j,i+1)}$ is accepted if $r > 0$. Otherwise, the search radius $d^{(i)}$ is reduced, and the iteration is repeated. The termination condition is $\|\mathbf{x}^{(i+1)} - \mathbf{x}^{(i)}\| < \varepsilon$ OR $d(i) < \varepsilon$, where ε is the required resolution of the search process (e.g., $\varepsilon = 10^{-3}$). The concept of iterative generation of the trade-off designs has been shown in Fig. 4.

2.4 Optimization Algorithm

The flow diagram of the proposed tolerance-aware MO procedure has been shown in Fig. 5. As mentioned earlier, the best nominal design \mathbf{x}^p is first identified, followed by the establishment of the target performance levels $P_{\max,j}$. The latter are determined using the assumed maximum acceptable performance level P_{\max} , $F_p(\mathbf{x}^p)$, and the number of designs N_p . The performance-robustness trade-off designs are then obtained by sequentially solving (13) as described in Section 2.3.

3 Verification Case Studies

This section provides numerical verification of the multi-objective optimization procedure of Section 2. It is based on two microstrip antennas, a dual-band dipole, and a quasi-Yagi structure. In both cases, the goal is to find the trade-offs between the nominal performance defined through maximum in-band reflection, and the robustness, defined as the maximum level of parameter deviations that still ensure 100-percent fabrication yield.

3.1 Case I: Dual-Band Dipole Antenna

Consider a dual-band dipole with truncated substrate [34] shown in Fig. 6(a), implemented on RO4003 substrate ($\varepsilon_r = 3.38$, $h = 0.81$ mm). The parameter vector is $\mathbf{x} = [L_{rr} \ d \ W_s \ W_d \ S \ L_d \ L_{gr} \ W_{gr}]^T$ (dimensions in mm, except the relative ones ending with the subscript r). Other parameters are: $W_r = 5$ mm, $L_s = 5$ mm, $L_0 = 25$ mm, $W_0 = 1.9$ mm, $L_r = L_{rr}((W_s - W_0)/2 - W_d - d)$, $L_g = L_{gr}(L_0 - W_{gr}/2 + W_0/2)$, $W_g = W_{gr}W_s$, and $g = W_d$. The EM model is implemented in CST Microwave Studio and evaluated using the time-domain solver.

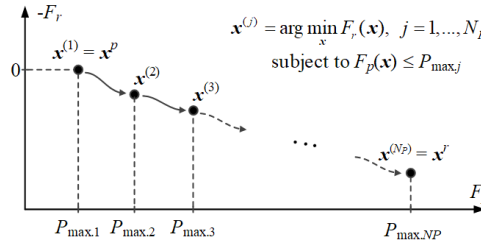


Fig. 4. Conceptual illustration of sequential generation of performance-robustness trade-off designs.

The target operating frequencies and bandwidths are $f_{01} = 3.5$ GHz, $f_{02} = 4.2$ GHz, and $B_1 = B_2 = 80$ MHz, respectively. The best nominal performance design is $\mathbf{x}^p = [0.91 \ 1.45 \ 48.01 \ 3.66 \ 1.80 \ 4.97 \ 1.00 \ 0.38]^T$. At this design, we have $F_p(\mathbf{x}^p) = -15.1$ dB, and $F_r(\mathbf{x}^p) = 0$ (cf. Section 2.1). Five more trade-off designs have been obtained, corresponding to $P_{\max,2} = -14$ dB, $P_{\max,3} = -13$ dB, through $P_{\max,6} = -10$ dB (the highest acceptable in-band reflection level), as shown in Table 1 and Fig. 6(b). Figure 7 visualizes EM-driven Monte Carlo (MC) simulation for the selected designs. MC confirms that the fabrication yield is indeed close to 100 percent for all pairs $\{F_p(\mathbf{x}^{(j)}), F_r(\mathbf{x}^{(j)})\}$. The actual yield is between 98 and 100 percent (design dependent), yet, it should be noted that MC itself is characterized by a relatively large yield estimation variance due to using only 500 samples. The proposed MO approach is computationally efficient. The average cost of generating one trade-off design is only about 62 EM simulations of the antenna structure, which is possible by utilization of the feature-based surrogates (cf. Section 2.2).

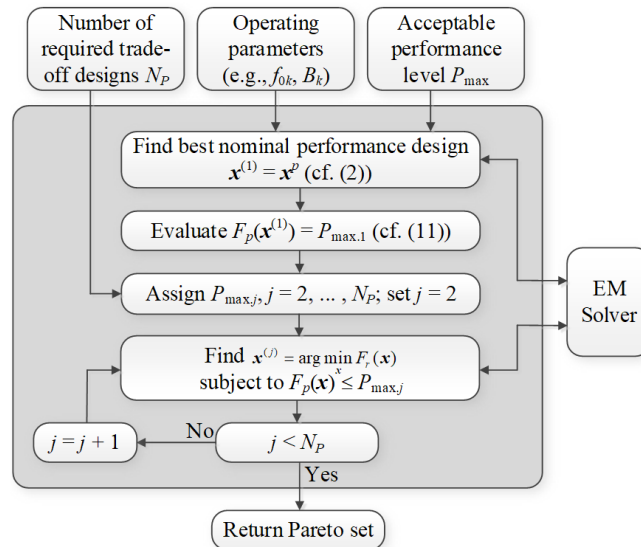


Fig. 5. Flow diagram of the proposed tolerance-aware multi-objective optimization algorithm using the feature-based regression surrogates and trust-region parameter adjustment process.

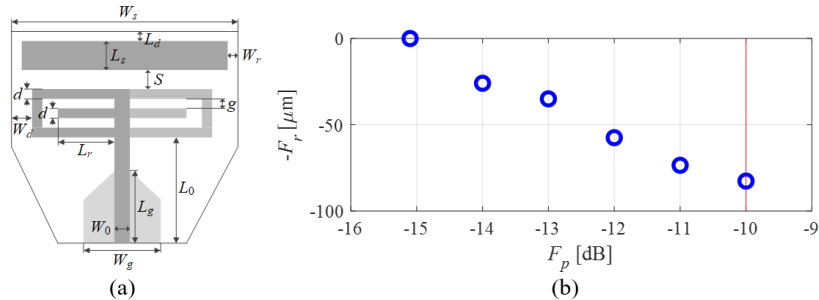


Fig. 6. Dual-band dipole antenna with truncated substrate [34]: (a) antenna geometry, the light-gray shade marks the ground plane, (b) performance-robustness trade-off designs obtained using the proposed procedure. The vertical line marks the maximum acceptable in-band reflection level.

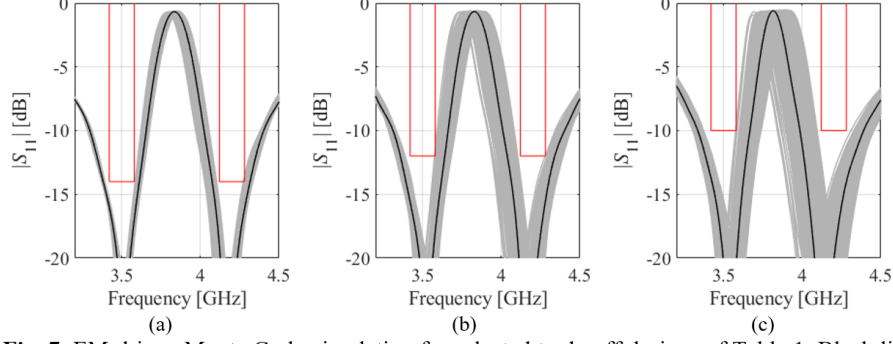


Fig. 7. EM-driven Monte Carlo simulation for selected trade-off designs of Table 1. Black line shows the antenna response at the given trade-off design: (a) design $\mathbf{x}^{(2)}$, (b) design $\mathbf{x}^{(4)}$, (c) design $\mathbf{x}^{(6)}$, grey lines correspond to 500 random observables generated according to the assumed probability distribution with the variance equal to F_r . Thin lines denote design specifications.

Table 1. Dual-band antenna of Fig. 6(a): results of multi-objective design with tolerances

Design	Objectives		Geometry parameters [absolute in mm, relative unitless]							
	F_p [dB]	F_r [μm]	L_{rr}	d	W_s	W_d	S	L_d	L_{gr}	W_{gr}
$\mathbf{x}^{(1)} = \mathbf{x}^*$	-15.1	0	0.91	1.45	48.01	3.66	1.80	4.97	1.00	0.38
$\mathbf{x}^{(2)}$	-14	25.9	0.92	1.42	47.99	3.62	1.78	4.93	1.00	0.38
$\mathbf{x}^{(3)}$	-13	35.0	0.92	1.40	47.99	3.65	1.80	4.95	1.00	0.38
$\mathbf{x}^{(4)}$	-12	57.5	0.92	1.34	47.98	3.72	2.01	4.68	0.99	0.39
$\mathbf{x}^{(5)}$	-11	73.5	0.92	1.24	47.87	3.65	2.32	4.58	0.99	0.38
$\mathbf{x}^{(6)} = \mathbf{x}^*$	-10	82.7	0.92	1.20	47.85	3.68	2.39	4.62	0.99	0.38

3.2 Case II: Quasi-Yagi Antenna

As the second example, consider a quasi-Yagi antenna with integrated balun [35], Fig. 8(a), implemented on RO4003 substrate ($\epsilon_r = 3.38$, $h = 1.5$ mm). The design parameters are $\mathbf{x} = [L_a L_b L_c L_d W w_a D_a D_b D_c D_{lr} D_{rr} S_r w_{br} w_{cr}]^T$ (subscript r marks the relative parameters). We also have $D_l = D_{lr}L_a$, $D_r = D_{rr}L_a$, $S = S_rW$, $w_b = w_{br}W/2$, $w_c = w_{cr}W$, $w_0 = 3.4$ mm. The EM model is implemented in CST Microwave Studio.

The center frequency and bandwidth are $f_{01} = 2.5$ GHz and $B_1 = 50$ MHz, respectively. Furthermore, the realized gain at 2.5 GHz is to be at least 7.9 (i.e., 8 dB with the tolerance of 0.1 dB). The best nominal performance design $\mathbf{x}^p = [20.21 \ 12.33 \ 16.47 \ 26.09 \ 52.06 \ 1.83 \ 1.02 \ 4.39 \ 4.26 \ 0.37 \ 0.44 \ 0.98 \ 0.71 \ 0.72]^T$ corresponds to $F_p(\mathbf{x}^p) = -17.0$ dB. Seven additional trade-off designs have been found, corresponding to $P_{\max,2} = -16$ dB, $P_{\max,3} = -15$ dB, through $P_{\max,7} = -10$ dB.

The results have been gathered in Table 2 and Fig. 8(b). Figure 9 visualizes EM-based Monte Carlo simulation for the selected trade-off designs. The average value of the estimated yield is 97 percent, which is sufficiently close to 100 given the challenging nature of the problem (fourteen parameters, and limited predictive power of the surrogate model for larger values of input tolerances). Again, the proposed algorithm exhibits excellent computational efficiency with the average cost of identifying the trade-off designs of only 82 EM simulations per point.

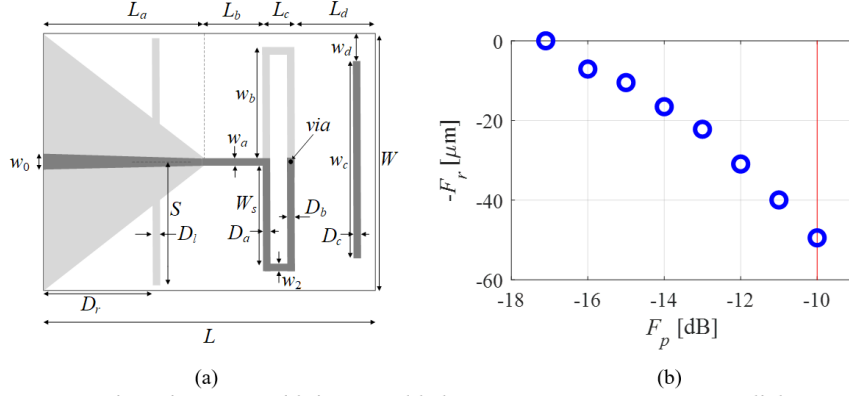


Fig. 8. Quasi-Yagi antenna with integrated balun [35]: (a) antenna geometry, light-gray shade indicates ground-plane metallization, (b) performance-robustness trade-off designs obtained using the proposed procedure for multi-objective optimization with tolerances. The vertical line marks the maximum acceptable in-band reflection level.

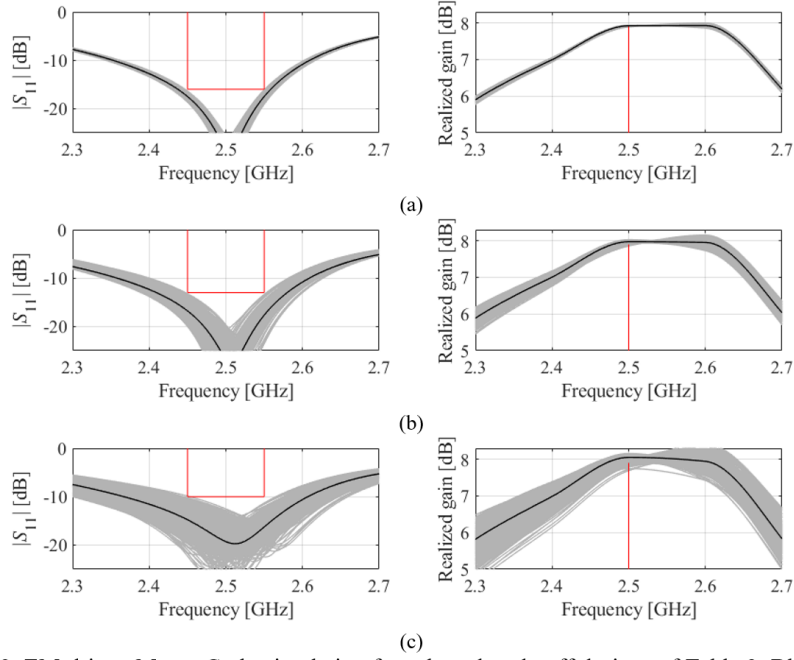


Fig. 9. EM-driven Monte Carlo simulation for selected trade-off designs of Table 2. Black line shows the antenna response at the given trade-off design: (a) design $\mathbf{x}^{(2)}$, (b) design $\mathbf{x}^{(5)}$, (c) design $\mathbf{x}^{(8)}$, grey lines correspond to 500 random observables generated according to the assumed probability distribution with the variance equal to F_r . Thin lines denote design specifications.

Table 2. Quasi-Yagi antenna of Fig. 8(a): results of multi-objective design with tolerances

Design	Objectives		Geometry parameters [absolute in mm, relative unitless]													
	F_p [dB]	F_r [μm]	L_a	L_b	L_c	L_d	W	w_a	D_a	D_b	D_c	D_{lr}	D_{rr}	S_r	w_{br}	D_a
1	-17	0	20.2	12.3	16.5	26.1	52.1	1.83	1.02	4.39	4.26	0.37	0.44	0.98	0.71	0.72
2	-16	7.1	20.2	12.3	16.5	26.0	52.1	1.73	1.02	4.34	4.15	0.38	0.44	0.98	0.71	0.72
3	-15	10.5	20.3	12.4	16.5	26.0	52.1	1.73	1.03	4.34	4.11	0.38	0.43	0.98	0.71	0.72
4	-14	16.6	20.2	12.4	16.5	26.0	52.1	1.64	1.02	4.36	4.04	0.38	0.40	0.99	0.71	0.72
5	-13	22.2	20.2	12.4	16.5	26.0	52.1	1.69	1.02	4.41	4.02	0.38	0.40	0.99	0.71	0.73
6	-12	30.9	20.3	12.4	16.5	26.0	52.1	1.66	1.01	4.48	4.06	0.37	0.40	0.98	0.71	0.73
7	-11	39.9	20.5	12.4	16.4	26.1	52.1	1.49	1.01	4.50	3.99	0.38	0.40	0.98	0.71	0.73
8	-10	49.5	20.6	12.5	16.3	26.1	52.1	1.45	1.01	4.50	3.98	0.35	0.40	0.97	0.71	0.73

4 Conclusions

This paper proposed a novel technique for multi-objective optimization of antenna structures with tolerance analysis. Our approach allows for low-cost identification of the designs representing the best possible trade-offs between the nominal performance and the robustness. The latter is understood as the maximum level of geometry parameter deviations for which the perfect (100-percent) fabrication yield is still attainable. The main algorithmic tool employed in the presented procedure is a feature-based regression surrogate, which enables rapid estimation of the yield. Numerical validation involving two microstrip antennas demonstrates both the reliability and computational efficiency of the proposed framework, with only a few dozens of EM analyses required to generate each trade-off design. The future work will focus on extending the range of applicability of the technique for higher-dimensional problems.

Acknowledgement

The authors would like to thank Dassault Systemes, France, for making CST Microwave Studio available. This work is partially supported by the Icelandic Centre for Research (RANNIS) Grant 206606 and by National Science Centre of Poland Grant 2020/37/B/ST7/01448.

References

1. Li, Y., Ding, Y., Zio, E.: Random fuzzy extension of the universal generating function approach for the reliability assessment of multi-state systems under aleatory and epistemic uncertainties. *IEEE Trans. Reliability*, **63**(1), 13–25 (2014)
2. Elias, B.B.Q., Soh, P.J., Al-Hadi, A.A., Akkaraekthalin, P.: Gain optimization of low-profile textile antennas using CMA and active mode subtraction method. *IEEE Access*, **9**, 23691–23704 (2021)
3. Zhang, Z., Chen, H., Jiang, F., Yu, Y., Cheng, Q.S.: A benchmark test suite for antenna S-parameter optimization. *IEEE Trans. Ant. Propag.*, Early Access (2021)

4. Koziel, S., Pietrenko-Dabrowska, A.: Robust parameter tuning of antenna structures by means of design specification adaptation. *IEEE Trans. Ant. Propag.*, Early Access, (2021)
5. Xu, Q., Zeng, S., Zhao, F., Jiao, R., Li, C.: On formulating and designing antenna arrays by evolutionary algorithms. *IEEE Trans. Ant. Propag.*, **69**(2), 1118–1129 (2021)
6. Al-Azza, A.A., Al-Jodah, A.A., Harackiewicz, F.J.: Spider monkey optimization: a novel technique for antenna optimization. *IEEE Antennas Wireless Propag. Lett.*, **15**, 1016–1019 (2016)
7. Darvish, A., Ebrahimzadeh, A.: Improved fruit-fly optimization algorithm and its applications in antenna arrays synthesis. *IEEE Trans. Antennas Propag.*, **66**(4), 1756–1766 (2018)
8. Koziel, S., Sigurdsson, A.T.: Multi-fidelity EM simulations and constrained surrogate modeling for low-cost multi-objective design optimization of antennas. *IET Microwaves Ant. Prop.*, **12**(13), 2025–2029 (2018)
9. Xiao, S., Liu, G.Q., Zhang, K.L., Jing, Y.Z., Duan, J.H., Di Barba, P., Sykulski, J.K.: Multi-objective Pareto optimization of electromagnetic devices exploiting kriging with Lipschitzian optimized expected improvement. *IEEE Trans. Magn.*, **54**(3), art. no. 7001704 (2018)
10. De Villiers, D.I.L., Couckuyt, I., Dhaene, T.: Multi-objective optimization of reflector antennas using kriging and probability of improvement. *Int. Symp. Ant. Prop.*, 985–986, San Diego, USA (2017)
11. Lv, Z., Wang, L., Han, Z., Zhao, J., Wang, W.: Surrogate-assisted particle swarm optimization algorithm with Pareto active learning for expensive multi-objective optimization. *IEEE J. Automatica Sinica*, **6**(3), 838–849 (2019)
12. Koziel, S., Ogurtsov, S.: Multi-objective design of antennas using variable-fidelity simulations and surrogate models. *IEEE Trans. Antennas Prop.*, **61**(12), 5931–5939 (2013)
13. Liu, Y., Cheng, Q.S., Koziel, S.: A generalized SDP multi-objective optimization method for EM-based microwave device design. *Sensors*, **19**(14), (2019)
14. Toktas, A., Ustun, D., Tekbas, M.: Multi-objective design of multi-layer radar absorber using surrogate-based optimization. *IEEE Trans. Microw. Theory Techn.*, **67**(8), 3318–3329 (2019)
15. Du, J., Roblin, C.: Stochastic surrogate models of deformable antennas based on vector spherical harmonics and polynomial chaos expansions: application to textile antennas. *IEEE Trans. Ant. Propag.*, **66**(7), 3610–3622 (2018)
16. Rayas-Sanchez, J.E., Gutierrez-Ayala, V.: EM-based statistical analysis and yield estimation using linear-input and neural-output space mapping. *IEEE MTT-S Int. Microwave Symp. Digest (IMS)*, 1597–1600 (2006)
17. Zhang, J., Zhang, C., Feng, F., Zhang, W., Ma, J., Zhang, Q.J.: Polynomial chaos-based approach to yield-driven EM optimization. *IEEE Trans. Microwave Theory Techn.*, **66**(7), 3186–3199 (2018)
18. Wu, Q., Chen, W., Yu, C., Wang, H., Hong, W.: Multilayer machine learning-assisted optimization-based robust design and its applications to antennas and arrays. *IEEE Trans. Ant. Prop.*, Early View (2021)
19. Abdel-Malek, H.L., Hassan, A.S.O., Soliman, E.A., Dakrouy, S.A.: The ellipsoidal technique for design centering of microwave circuits exploiting space-mapping interpolating surrogates. *IEEE Trans. Microwave Theory Techn.*, **54**(10), 3731–3738 (2006)
20. Ma, B., Lei, G., Liu, C., Zhu, J., Guo, Y.: Robust tolerance design optimization of a PM claw pole motor with soft magnetic composite cores. *IEEE Trans. Magn.*, **54**(3), art. no. 8102404 (2018)

21. Ren, Z., He, S., Zhang, D., Zhang, Y., Koh, C.S.: A possibility-based robust optimal design algorithm in preliminary design state of electromagnetic devices. *IEEE Trans. Magn.*, **52**(3), art. no. 7001504 (2016)
22. Spina, D., Ferranti, F., Antonini, G., Dhaene, T., Knockaert, L.: Efficient variability analysis of electromagnetic systems via polynomial chaos and model order reduction. *IEEE Trans. Comp. Packaging Manufacturing Techn.*, **4**(6), 1038–1051 (2014)
23. Pietrenko-Dabrowska, A., Koziel, S., Al-Hasan, M.: Expedited yield optimization of narrow- and multi-band antennas using performance-driven surrogates. *IEEE Access*, **8**, 143104–143113 (2020)
24. Xia, B., Ren, Z., Koh, C.S.: Utilizing Kriging surrogate models for multi-objective robust optimization of electromagnetic devices. *IEEE Trans. Magn.*, **50**(2), art. no. 7017104 (2014)
25. Liu, B., Aliakbarian, H., Ma, Z., Vandenbosch, G.A., Gielen, G., Excell, P.: An efficient method for antenna design optimization based on evolutionary computation and machine learning techniques. *IEEE Trans. Antennas Propag.*, **62**, 7–18 (2014)
26. Easum, J.A., Nagar, J., Werner, P.L., Werner, D.H.: Efficient multi-objective antenna optimization with tolerance analysis through the use of surrogate models. *IEEE Trans. Ant. Prop.*, **66**(12), 6706–6715 (2018)
27. K. Deb, *Multi-Objective Optimization Using Evolutionary Algorithms*. Wiley, New York, (2001)
28. Hassan, A.S.O., Abdel-Malek, H.L., Mohamed, A.S.A., Abuelfadl, T.M., Elqenawy, A.E.: Statistical design centering of RF cavity linear accelerator via non-derivative trust region optimization. *IEEE Int. Conf. Numerical EM Multiphysics Modeling Opt. (NEMO)*, 1–3 (2015)
29. Koziel, S.: Fast simulation-driven antenna design using response-feature surrogates. *Int. J. RF & Microwave CAE*, **25**(5), 394–402 (2015)
30. Pietrenko-Dabrowska, A., Koziel, S.: Fast design closure of compact microwave components by means of feature-based metamodels. *Electronics*, **10**(1), art. no. 10 (2021)
31. Pietrenko-Dabrowska, A., Koziel, S.: Simulation-driven antenna modeling by means of response features and confined domains of reduced dimensionality. *IEEE Access*, **8**, 228942–228954 (2020)
32. Press, W.H., Teukolsky, S.A., Vetterling, W.T., Flannery, B.P.: Golden section search in one dimension. In *Numerical Recipes: The Art of Scientific Computing* (3rd ed.), Cambridge University Press, New York (2007)
33. Conn, A.R., Gould, N.I.M., Toint, P.L., *Trust Region Methods*, MPS-SIAM Series on Optimization (2000)
34. Qudrat-E-Maula, M., Shafai, L.: A dual band microstrip dipole antenna,” *Int. Symp. Ant. Technology and Applied Electr. (ANTEM)*, 1–2, Victoria, BC, Canada, July 13-16 (2014)
35. Farran, M., Boscolo, S., Locatelli, A., Capobianco, A.D., Mirio, M., Ferrari, V., Modotto, D.: Compact quasi-Yagi antenna with folded dipole fed by tapered integrated balun. *Electronics Letters*, **52**(10), 789–790 (2016)